J. Chem. Sci. Vol. 126, No. 3, May 2014, pp. 701–710.

Second harmonic generation and electro-optical Pockels effect of 1- and 3-nitro-6-azabenzo[*a*]pyrene *N*-oxide isomers: A Hartree–Fock and Coulomb-attenuating density functional theory investigation

ANDREA ALPARONE

Department of Chemistry, University of Catania, viale A. Doria 6, Catania 95125, Italy
e-mail: agalparone@gmail.com; agalparone@unict.it

MS received 6 September 2013; revised 18 November 2013; accepted 20 November 2013

Abstract. Structural, energetic, spectroscopic, linear and nonlinear optical (NLO) properties of the environmental mutagens 1- and 3-nitro-6-azabenzo[*a*]pyrene *N*-oxides were characterized by means of Hartree–Fock as well as B3LYP and CAM-B3LYP density functional theory computations. The NLO investigations were performed for the second harmonic generation (SHG) and electro-optical Pockels effect (EOPE) at the incident wavelength of 1064 nm. The results show that, the predicted structures, vibrational spectra, nucleus independent chemical shifts, ionization energy, electron affinity as well as electronic polarizabilities are little influenced by the position of the nitro substituent. Differently, the dipole moment (μ) and the first-order hyperpolarizabilities (β_μ) are significantly dependent on the isomerization. The rather different mutagenic activity of the investigated isomers could be related to their diverse polarity. At the CAM-B3LYP level, when passing from the 1- to the 3-nitro-6-azabenzo[*a*]pyrene *N*-oxide isomer, the μ datum increases by about 5 D (a factor of three), whereas the static and dynamic β_μ values decrease by ca. 50%. Dipole moment measurement and SHG and EOPE NLO techniques are potentially useful to distinguish these important environmental mutagens.

Keywords. 1-, 3-Nitro-6-azabenzo[*a*]pyrene *N*-oxide; nitro-polycyclic aromatic hydrocarbons; dipole moment; (hyper)polarizabilities; SHG and EOPE NLO phenomena; HF and DFT computations.

1. Introduction

Nitro-azabenzo[*a*]pyrene *N*-oxides (**NNO**s, figure 1) are nitro-polycyclic aromatic hydrocarbons (NPAHs) of great interest from environmental and toxicological viewpoints.[1–3] As widely documented in literature, NPAHs are persistent and widespread organic contaminants, mainly originating from direct combustion processes or reactions between PAHs and NO_x.[4–7] The presence of NPAHs in atmospheric environments is significantly lower than that of their unsubstituted parents.[8] However, NPAH pollutants often exhibit noticeably higher levels of mutagenic and carcinogenic activities than those of the PAH congeners.[9,10]

The **NNO**s which are present in the airborne particulate matter, are predicted to be mutagenic agents and their chemical properties are significantly influenced by the *N*-oxidation of the azabenzene ring.[1–3] They are principally formed during diesel exhausts[3] and as for other NPAHs,[11] their mutagenic activities are remarkably affected by the position of the nitro substituent.[1,2] Indeed, considering the *Salmonella typhimurium* mutation test accomplished with the TA98, TA98NR, YG1021 and YG1024 microbial strains, the mutagenic activity of 3-nitro-6-azabenzo[*a*]pyrene *N*-oxide (**3NNO**) is predicted to be ca. one order of magnitude higher than that of the 1-nitro-6-azabenzo[*a*]pyrene *N*-oxide (**1NNO**) isomer.[1,2] Therefore, the characterization of their physicochemical properties is of essential importance for the identification and removal from contaminated areas. Some fundamental molecular properties for 3-nitro-6-azabenzo[*a*]pyrene and its *N*-oxide derivative (**3NNO**) have been recently determined through accurate quantum chemical calculations.[12]

In the present work, we have extended our computational investigation to the **1NNO** isomer by using *ab initio* Hartree–Fock (HF) and density functional theory (DFT) methods. Besides to the geometries, energies, IR and Raman spectra, NMR parameters, dipole moments and electronic polarizabilities, herewith for the first time we report the static and frequency-dependent electronic first-order hyperpolarizabilities. The main goal of this study is to characterize and identify physicochemical properties useful to discriminate **1NNO** from **3NNO**. The electronic first-order hyperpolarizabilities and the related nonlinear optical (NLO) second harmonic generation (SHG) and electro-optical Pockels effect (EOPE) properties can be significantly affected

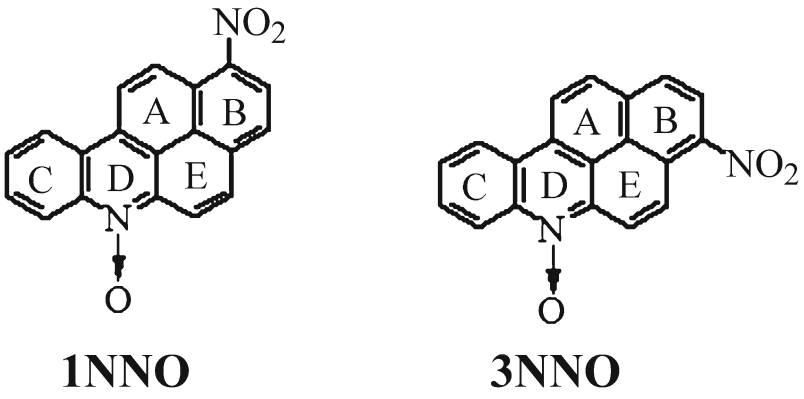

Figure 1. Molecular structures of 1- and 3-nitro-6-azabenzo[*a*]pyrene *N*-oxide isomers.

by structural features, being potentially helpful to distinguish isomeric forms.[13–17] In addition, Katritzky and co-workers recently have proposed the electronic first-order hyperpolarizability as possible molecular descriptor for QSPR applications.[18]

The paper is organized as follows. In section 2, a description of the employed computational methods is given; in section 3, the results on geometries, energetics, spectroscopic properties as well as on electronic properties are presented; in section 4, conclusive comments are provided.

2. Computational details

The gas phase geometry of **1NNO** in the neutral ground-state was optimized using the B3LYP functional[19,20] with the 6-31G* basis set[21] (B3LYP/6-31G*). Infrared and Raman spectra of **1NNO** were obtained under the harmonic approximation at the B3LYP/6-31G* level on the geometry optimized at the same level. The investigated structure is a stationary point on the potential energy surface (no imaginary wavenumbers).

On the B3LYP/6-31G* geometry we computed the nucleus independent chemical shifts (NICSs)[22] for each one of the five aromatic rings of **1NNO** using the Coulombic-attenuating DFT method (CAM-B3LYP)[23] and the 6-31+G* basis set.[21] Specifically, we evaluated the NICS value perpendicular to the plane of the ring at the distance of 1 Å [NICS(1)$_{yy}$]. Recent investigations have demonstrated that NICS(1)$_{yy}$ is an adequate parameter to predict the local aromaticity for PAHs.[22,24,25]

Dipole moments (μ), static and dynamic electronic polarizabilities (α) and first-order hyperpolarizabilities (β) of the investigated isomers were computed using the HF and CAM-B3LYP levels on the B3LYP/6-31G* geometries. The CAM-B3LYP μ and α data of **3NNO** were taken from ref. 12, whereas the β values of both the **NNO** isomers were determined in the present work. The long-range corrected CAM-B3LYP functional is recognized to be a suitable method for (hyper)polarizability computations, often reproducing accurately the results obtained with correlated *ab initio* levels and with performances superior to those obtained by the traditional DFT methods.[26–30] The electric property calculations were thoroughly carried out with the polarised and diffuse 6-31+G* basis set. This basis set has been proven to be sufficiently adequate for (hyper)polarizability calculations, giving good results when compared to those obtained with much more extended basis sets, but with significantly minor CPU demands.[31,32] The frequency-dependent polarizabilities [$\alpha(-\omega;\omega)$] and first-order hyperpolarizabilities for the NLO SHG [$\beta(-2\omega;\omega;\omega)$] and EOPE [$\beta(-\omega;\omega;0)$] phenomena were computed at the characteristic Nd:YAG laser wavelength of 1064 nm ($\hbar\omega = 0.04282$ a.u.). The static and dynamic (hyper)polarizabilities were calculated analytically through the Coupled-Perturbed HF theory,[33,34] as second and third derivatives of energy (E) with respect to Cartesian components of electric field strength (F):

$$E(F) = E(0) - \sum_i \mu_i F_i - \frac{1}{2}\sum_{ij} \alpha_{ij} F_i F_j - \frac{1}{6}\sum_{ijk} \beta_{ijk} F_i F_j F_k \ldots, \quad (1)$$

$$\alpha_{ij} = -\left[\frac{\partial^2 E(F)}{\partial F_i \partial F_j}\right]_{F\to 0}, \quad \beta_{ijk} = -\left[\frac{\partial^3 E(F)}{\partial F_i \partial F_j \partial F_k}\right]_{F\to 0}. \quad (2)$$

Besides to the μ_i, α_{ij} and β_{ijk} components we report the commonly used invariant quantities, dipole

moment (μ) average polarizability (<α>), polarizability anisotropy ($\Delta\alpha$) and first-order hyperpolarizability aligned along the direction of the molecular dipole moment (β_μ),which are defined as follows:

$$\mu = \sqrt{\mu_x^2 + \mu_y^2 + \mu_z^2}, \tag{3}$$

$$< \alpha >= \frac{1}{3}\left(\alpha_{xx} + \alpha_{yy} + \alpha_{zz}\right), \tag{4}$$

$$\Delta\alpha = \left\{\frac{1}{2}\left[\left(\alpha_{xx} - \alpha_{yy}\right)^2 + \left(\alpha_{xx} - \alpha_{zz}\right)^2 + \left(\alpha_{yy} - \alpha_{zz}\right)^2 + 6\left(\alpha_{xy}^2 + \alpha_{xz}^2 + \alpha_{yz}^2\right)\right]\right\}^{\frac{1}{2}}, \tag{5}$$

$$\beta_\mu = \sum_{i=x,y,z} \beta_i \mu_i / |\mu|. \tag{6}$$

where $\beta_i (i = x, y, z)$ is given by, $\beta_i = \frac{1}{3} \sum_{j=x,y,z} \left(\beta_{ijj} + \beta_{jij} + \beta_{jji}\right)$,

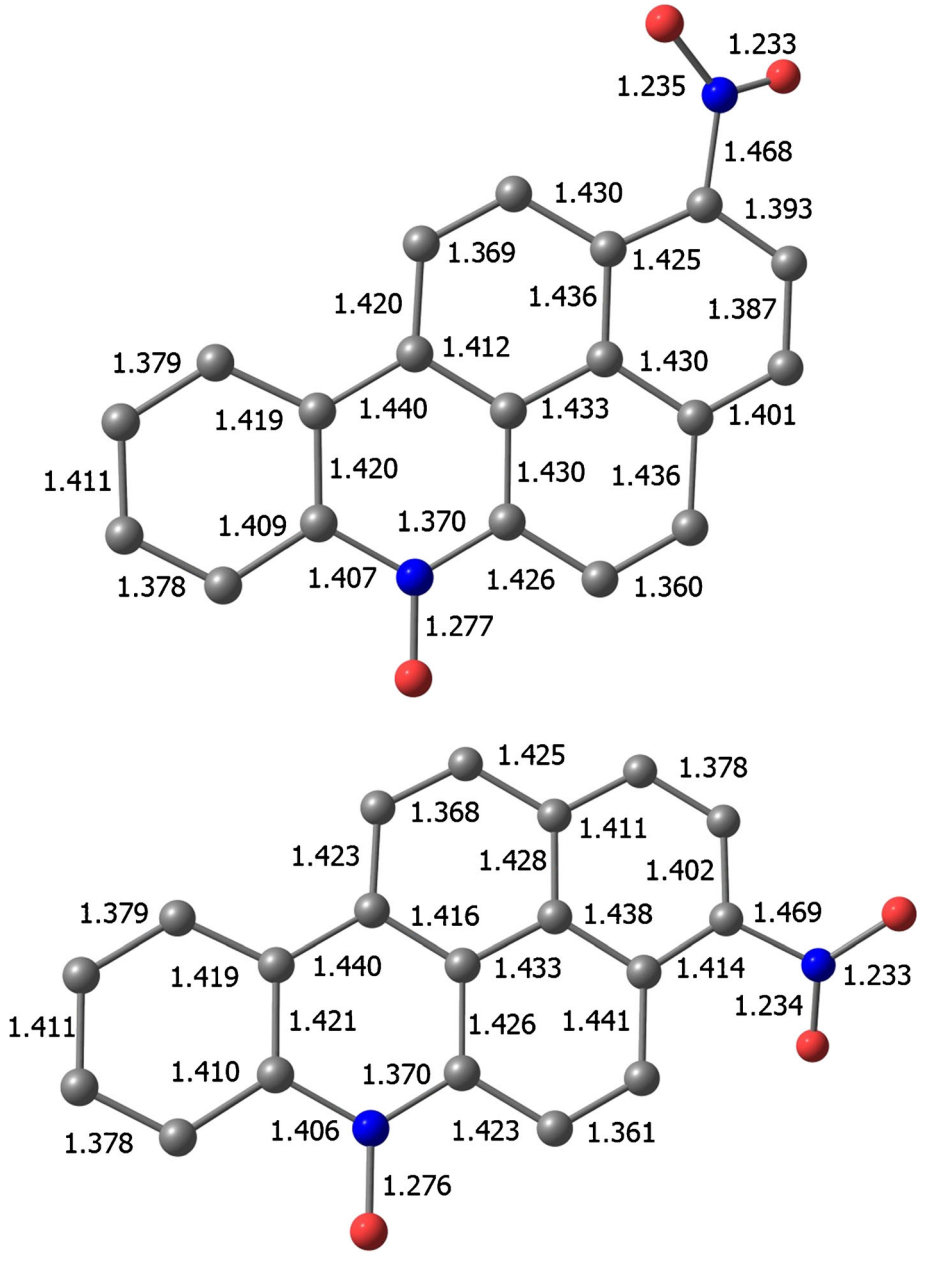

Figure 2. Selected bond lengths/Å of **1NNO** and **3NNO**. B3LYP/6-31G* results. The data of the **3NNO** isomer were taken from ref. 12.

For the response electric properties atomic units are used throughout the work. Conversion factor to the SI are: 1 a.u. of α ($e^2a_0^2E_h^{-1}$) = 1.648778×10^{-41} C^2 m^2 J^{-2}; 1 a.u. of β ($e^3a_0^3E_h^{-2}$) = 3.206361×10^{-53} C^3 m^3 J^{-2}. All computations were performed with the GAMESS[35] and GAUSSIAN 09[36] programs.

3. Results and discussion

3.1 *Energies, geometries and spectroscopic properties*

The recently published structural and spectroscopic data of the **3NNO** isomer were taken from ref. 12. At the B3LYP/6-31G* level, the title compounds are almost iso-energetic, the **3NNO** isomer being predicted to lie 0.42 kcal/mol above the **1NNO** structure. Figure 2 reports the B3LYP/6-31G* CC, CN and NO bond lengths for **1NNO** and **3NNO**.[12] The B3LYP/6-31G* computations predict for the **NNO** isomers almost similar bond lengths (a similar situation is found for the bond angles, which are not reported here and are available on request from the author), the largest differences not surprisingly, occurring for the ring A (figure 1). In addition, the characteristic O–N–C–C dihedral angles, which deviate from the planarity, are rather close, being calculated to be 22.0° and 20.8° for **1NNO** and 22.6° and 24.1° for **3NNO**.[12]

In figure 3 are displayed the IR and Raman spectra of **1NNO** and **3NNO**,[12] calculated at the B3LYP/6-31G* level. As usually adopted in literature, the harmonic wavenumbers were corrected for a single scaled factor (0.9594) previously reported by Irikura *et al.*[37] The most important vibrational transitions of **3NNO** have been recently assigned,[12] thus here we briefly discuss only the most relevant spectral differences between the investigated isomers. As can be appreciated from figure 3, in the highest-energy region (wavenumbers > 3000 cm^{-1}), the IR and Raman spectra are exclusively characterized by C-H stretching peaks, with spectral profiles slightly influenced by the structure. The vibrational spectra between 1000 and 1700 cm^{-1}, which involve vibrations mainly localised on the rings and NO_2 substituent, are marginally affected by the structural features, in some consistency with the calculated geometrical parameters, and are of little utility for the spectroscopic identification of the **NNO** isomers. In particular, the IR spectra of both the isomers are dominated by a transition mainly attributed to the symmetrical stretching of the NO_2 group + C–N stretching + rings stretching mode. It is located at 1315 cm^{-1} for **1NNO** and at 1318 cm^{-1} for **3NNO**,[12] with similar intensity values for both the isomers

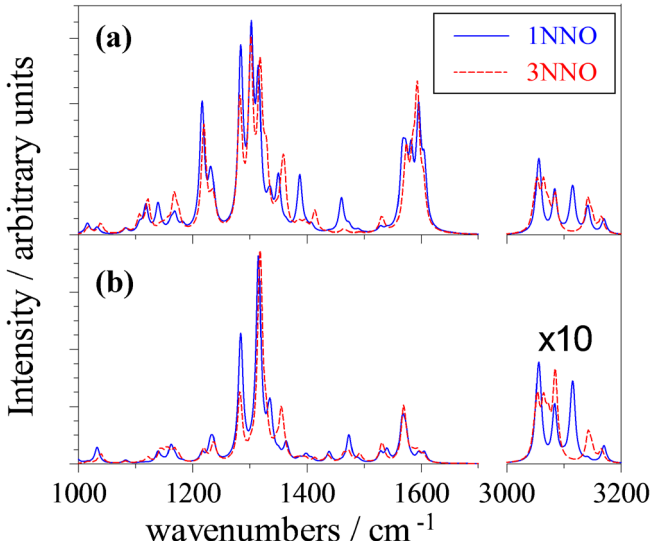

Figure 3. Calculated Raman (**a**) and IR (**b**) spectra of **1NNO** and **3NNO**. Pure Lorentzian band shapes with a full width at half maximum of 10 cm^{-1} were used. B3LYP/6-31G* results. The wavenumbers were corrected by a single scaling factor of 0.9594. The IR intensities of the bands in the wavenumbers range between 3000 and 3200 cm^{-1} were magnified by a factor of 10. The data of the **3NNO** isomer were taken from ref. 12.

(ca. 14 $D^2Å^{-2}amu^{-1}$). The most intense Raman peak (with a Raman activity of ca. 1100 $Å^4amu^{-1}$), ascribed to a ring stretching vibration is placed at 1303 and 1302 cm^{-1} for **1NNO** and **3NNO**,[12] respectively. The above findings are also confirmed by the calculated $NICS(1)_{yy}$ values (figure 4), with small differences between the studied isomers (within 0.0–0.9 ppm, 0–9%). The lowest-wavenumber IR and Raman regions (wavenumbers < 1000 cm^{-1}, here not displayed) show relatively weak peaks, being little informative to discriminate the investigated isomers.

Oxidation and/or reduction reactions of NPAHs have been often hypothesized to be crucial steps in the mutagenic activation pathways.[4,5,38] Oxidation and reduction properties are usually estimated by vertical ionization energy (VIE) and vertical electron affinity (VEA), respectively. To this purpose we performed ΔSCF calculations for **1NNO** using CAM-B3LYP/6-31+G* computations on the geometry of the neutral ground-state.[12] The ΔSCF VIE and VEA values of **3NNO** have been recently calculated at the same level of theory.[12] To the best of our knowledge, the observed

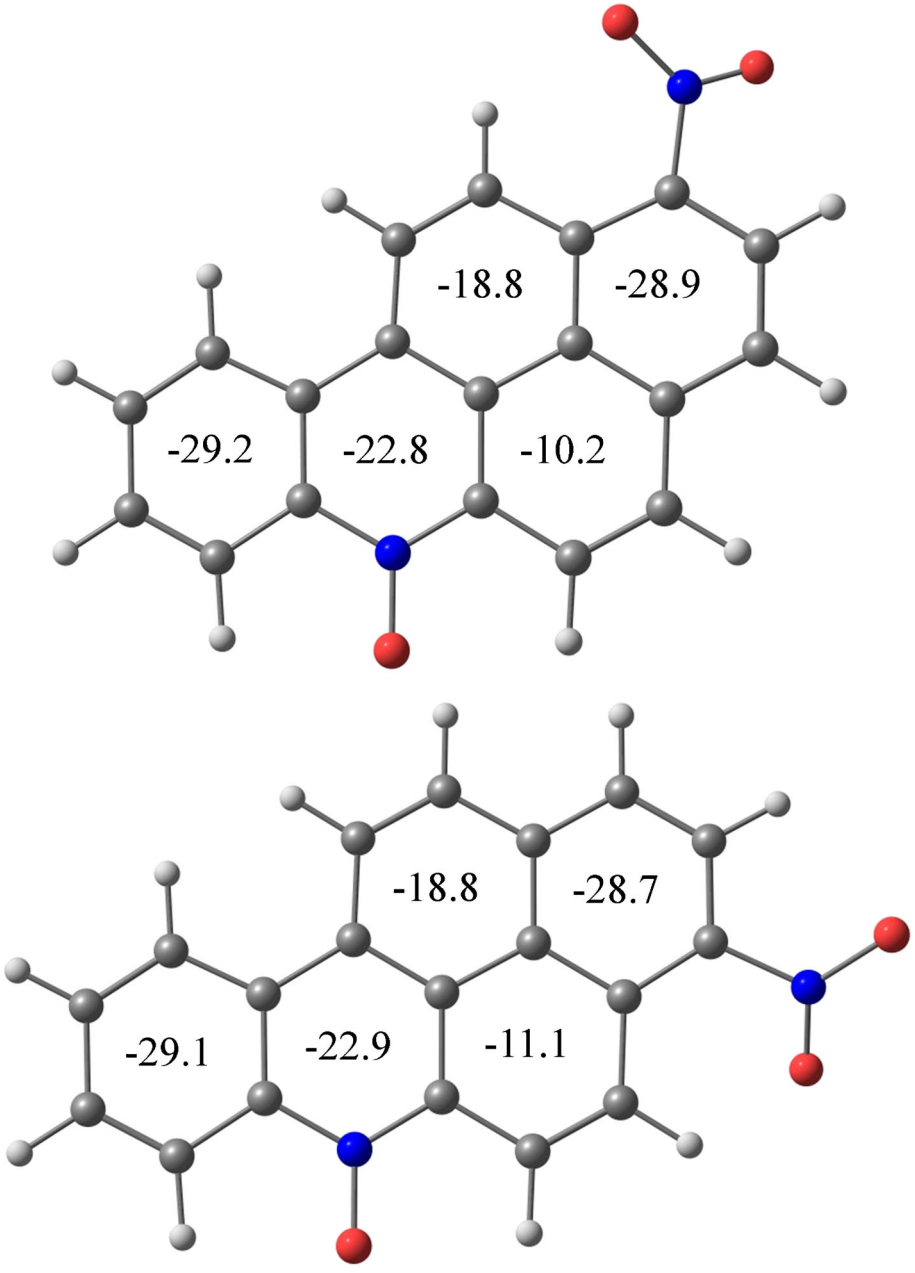

Figure 4. Calculated CAM-B3LYP/6-31+G* $NICS(1)_{yy}$ values/ppm of **1NNO** and **3NNO.** The data of the **3NNO** isomer were taken from ref. 12.

VIE and VEA values for **NNO**s are unavailable so far. The ΔSCF-CAM-B3LYP/6-31+G* method has been recently employed with success to evaluate the VIE and VEA values of glycine[39] and of the related compound nitrobenzene,[12] for which experimental data are known. The CAM-B3LYP/6-31+G* VIE value for the **1NNO** isomer is predicted to be 7.24 eV, to be compared with the corresponding datum for **3NNO** of 7.23 eV.[12] Additionally, the calculated VEA values of the **NNO** isomers are both positive and close to each other, being calculated to be 2.11 eV (**1NNO**) eV and 2.07 eV (**3NNO**).[12] It is worth noting that, these results are in qualitatively agreement with the experimental electrochemical first reduction potentials obtained by cyclic voltammetry measurements which are −657 mV for **1NNO** and −665 nm for **3NNO**.[1] Thus, the close VIE and VEA values for the **NNO** isomers suggest that reduction and/or oxidation mechanisms are not sufficient to explain their somewhat different mutagenic activities. Note that the (VEA-VIE)/2 molecular hardness (η),[40,41] a physicochemical parameter frequently employed to estimate the order of stability of isomers, herewith calculated at the CAM-B3LYP/6-31+G* level, is almost the same for the **NNO** isomers (ca. 2.6 eV), in agreement with their calculated relative stability.

3.2 *Dipole moments and electronic (hyper)polarizabilities*

Dipole moments and electronic polarizabilities describe the permanent and induced charge distributions of molecules, characterizing intermolecular interactions via electrostatic, inductive and dispersive forces. Intermolecular forces are involved in the formation of enzyme-substrate complexes, which is presumed to be a fundamental step in the mutagenic activation mechanisms of NPAHs.[38] Enzyme-substrate forces have been often modelled by electric properties.[42–46]

Table 1 collects the μ and static α values for the **1NNO** and **3NNO** isomers obtained at the HF/6-31+G* and CAM-B3LYP/6-31+G* levels. The results show that both the magnitude and direction of the μ vector are strongly affected by the **1NNO** ↔ **3NNO** isomerisation (figure 5). Indeed, when passing from **1NNO** to **3NNO**, the CAM-B3LYP/6-31+G* (HF/6-31+G*) μ value increases by ca. 5 D (7 D), which corresponds to a factor of three (four). For the **1NNO** isomer the polar NO_2 and N→O groups are roughly anti-parallel to each other and the resulting dipolar contributions almost cancel to each other (μ is ca. 2–3 D). On the other hand, for the **3NNO** isomer, the mutual disposition of the NO_2 and N→O groups

Table 1. Dipole moments μ (D) and static (hyper)polarizabilities α (a.u.) and β (a.u.) of 1- and 3-nitro-6-azabenzo[*a*]pyrene *N*-oxides.[a]

	1NNO		**3NNO**	
	HF	CAM-B3LYP	HF	CAM-B3LYP[b]
μ_x	−1.77	−2.17	−6.02	−6.10
μ_y	0.13	0.11	−0.13	−0.12
μ_z	−1.07	−1.75	6.33	5.21
μ	2.08	2.79	8.74	8.02
α_{xx}	400.9	417.3	430.8	460.2
α_{yy}	111.5	111.5	112.1	112.0
α_{zz}	327.9	351.3	296.7	306.2
$<\alpha>$	280.1	293.4	279.9	292.8
$\Delta\alpha$	303.0	322.3	304.6	325.1
β_{xxx}	−358	−497	−1730	−2905
β_{yyy}	−3	−3	3	4
β_{zzz}	−2179	−2619	−740	−411
β_x	−1398	−1823	−1925	−2926
β_y	39	44	−52	−50
β_z	−2504	−3174	−971	−625
β_μ	2480	3410	623	1820

[a]Basis set: 6-31+G*. The calculations were carried out on the B3LYP/6-31G* geometry
[b]The dipole moment and polarizability values were taken from ref. 12

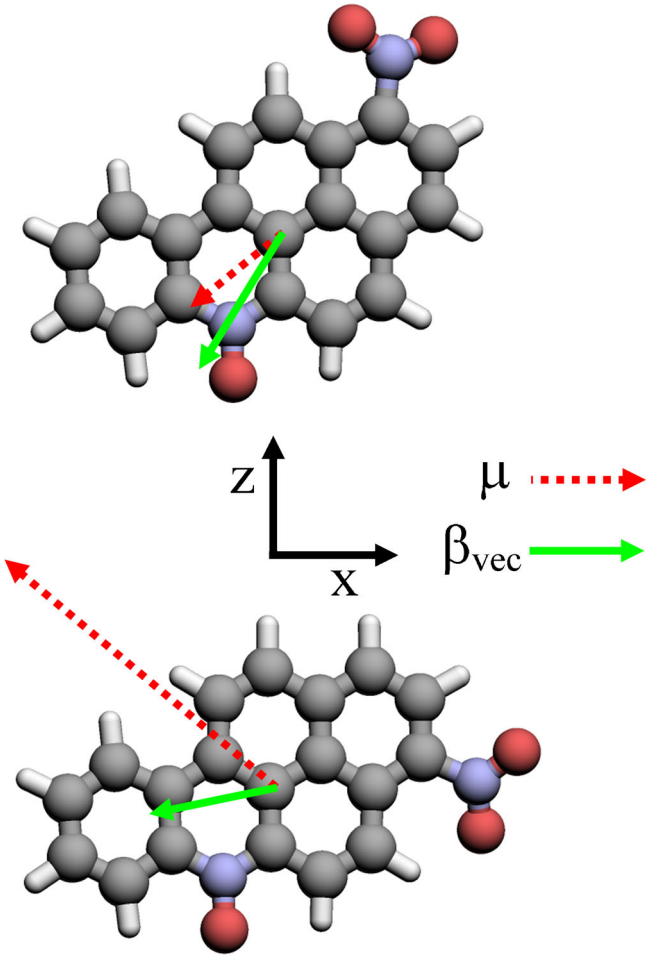

Figure 5. Dipole moment (μ) and first-order hyperpolarizability (β_{vec}) vectors of **1NNO** and **3NNO**. CAM-B3LYP/6-31+G* results.

constructively contributes to the relatively higher dipole moment (figure 5). As a consequence, in polar media the relative stability of the studied isomers is expected to decrease or even to be reversed. It is interesting to note that the more polar isomer (**3NNO**) is contemporarily the more mutagenic isomer. A similar behaviour, has been previously noticed for other NPAH series of isomers, such as nitronaphthalenes,[47] nitroanthracenes and nitrophenanthrenes,[48] mononitrobenzo[*a*]pyrenes[49] and dinitrobenzo[*a*]pyrenes.[50] Thus, the rather diverse polarity for the **NNOs** could be linked to their different mutagenicity.[47–50] On the basis of intermolecular electrostatic forces, in comparison to the **1NNO** isomer, **3NNO** is expected to be a stronger

Table 2. Frequency-dependent (hyper)polarizabilities $\alpha(-\omega;\omega)$ (a.u.) and $\beta(-\omega_\sigma;\omega_1,\omega_2)$ (a.u.) of 1- and 3-nitro-6-azabenzo[*a*]pyrene *N*-oxides.[a]

	1NNO		**3NNO**[b]	
$\hbar\omega$	0	0.04282	0	0.04282
$<\alpha>(-\omega;\omega)$	293.4	309.2	292.8	307.9
$\Delta\alpha(-\omega;\omega)$	322.3	355.4	325.1	356.5
$\beta_\mu(-\omega;\omega;0)$	3410	5000	1820	2606
$\beta_\mu(-2\omega;\omega;\omega)$	3410	16782	1820	6955

[a]CAM-B3LYP/6-31+G*//B3LYP/6-31G* results
[b]The polarizability values were taken from ref. 12

substrate for enzymes participating to the mutagenic activation processes.

At variance from the calculated μ data, the α values of the **NNO** isomers are much more closer to each other. Indeed, the static CAM-B3LYP/6-31+G* $<\alpha>$ and $\Delta\alpha$ values of **1NNO** are calculated to be 293.4 and 322.3 a.u., respectively, which are only 0.2 and 0.9% apart from the corresponding data of the **3NNO** isomer.[12] These findings agree with the predicted hardness values, η(**1NNO**) $\sim$ η(**3NNO**), the maximum hardness/minimum polarizability principles[40,51] being operative for these isomers. The largest polarizability component for both the **NNO**s lies along the longest x-axis (α_{xx}, figure 5), and recovers ca. 50% of the total polarizability ($\alpha_{xx} + \alpha_{yy} + \alpha_{zz}$). In agreement with the recent literature,[26–29,52–55] the HF/6-31+G* $<\alpha>$ and $\Delta\alpha$ values underestimate the CAM-B3LYP/6-31+G* data by 5–6%. The effects of the dispersion on the polarizabilities were here evaluated at the typical Nd:YAG laser wavelength (λ) of 1064 nm. The results are summarized in table 2. Resonance enhancement effects are expected to be negligible, since the used λ value is rather far from the observed lowest-energy absorptions at 463 nm (**1NNO**) and 466 nm (**3NNO**).[1] For both the isomers, the frequency-dependent $<\alpha>$ and $\Delta\alpha$ values increase the static figures by ca. 5 and 10%, respectively.

Besides to the μ_j and α_{jj} data, table 1 also includes the static β_{jjj} components. In comparison to the electronic polarizabilities, the β_μ values are much more influenced by the theoretical method and position of the NO_2 substituent. In fact, when passing from the HF/6-31+G* to the CAM-B3LYP/6-31+G* level, the static β_μ values of **1NNO** and **3NNO** increase by ca. 40 and 200%, respectively. More importantly, in opposition to the calculated μ values, the present results show that, β_μ(**1NNO**) > β_μ(**3NNO**) by ca. a factor of four (HF/6-31+G*) and two (CAM-B3LYP/6-31+G*). The above β_μ variations principally originate from the different magnitude and sign of the largest μ_j and β_j components lying along the x- and z-axis. In particular, on the basis of the highest-level computations (CAM-B3LYP/6-31+G*), the $\mu_x\beta_x/|\mu|$ value is positive for both the isomers (in parentheses is reported the percentage contribution to the β_μ value), being 1418 a.u. (+41.6%) for **1NNO** and 2226 a.u. (+122.3%) for **3NNO**. By contrast, the $\mu_z\beta_z/|\mu|$ value is positive for **1NNO** (+1991 a.u., +58.4%), whereas it is negative for **3NNO** (−406 a.u., −22.3%), owing to the opposite sign of the μ_z (+5.21 D) and β_z (−625 a.u.) values. As a consequence, the $\beta_\mu$difference between **1NNO** and **3NNO** is mainly attributable to the different contribution of the $\mu_z\beta_z/|\mu|$ term, which approximately lies along the N→O bond of the azabenzene unit. However, it is worth to mention that, when we take into account for the intrinsic first-order hyperpolarizability, as expressed by the quantity, $\beta_{vec} = \sqrt{\beta_x^2 + \beta_y^2 + \beta_z^2}$, the data for **1NNO** and **3NNO** isomers are much more close to each other (figure 5). Indeed at the CAM-B3LYP/6-31+G* level β_{vec}(**1NNO**) = 3661 a.u. and β_{vec}(**3NNO**) = 2992 a.u.

In order to qualitatively explore the spatial contributions of the electrons to the most important β_{jjj}, components, we performed an hyperpolarizability density analysis.[56–58] The calculations of the β densities [$\rho^{(2)}$(r)] were carried out following the procedure previously illustrated by Nakano and co-workers:[56–58]

$$\rho(r, F) = \rho^{(0)}(r) + \sum_j \rho_j^{(1)}(r)F_j + \frac{1}{2!}\sum_j \rho_{jk}^{(2)}(r)F_jF_k + \frac{1}{3!}\sum_j \rho_{jkl}^{(3)}(r)F_jF_kF_l + ..., \quad (7)$$

$$\beta_{ijk} = -\frac{1}{2!}\int r\rho_{jk}^{(2)}(r)dr, \quad (8)$$

$$\rho_{jk}^{(2)}(r) = \frac{\partial^2\rho(r, F)}{\partial F_j \partial F_k}\Big|_{F_j=0, F_k=0}. \quad (9)$$

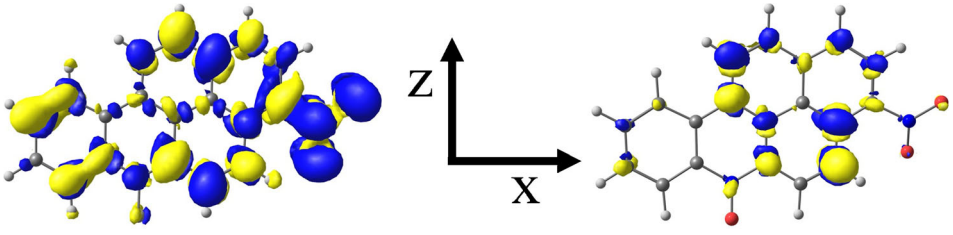

β_{xxx} = –2905 a.u. β_{zzz} = –411 a.u.

Figure 6. Hyperpolarizability density distributions $\rho_{xx}^{(2)}(r)$ (left) and $\rho_{zz}^{(2)}$(r) (right) of the **3NNO** tautomer. The yellow and blue surfaces refer to positive and negative $\rho_{jj}^{(2)}$(r) densities, respectively, computed at the iso-surface of 10 a.u.. CAM-B3LYP/6-31+G* results.

For a pair of localized positive and negative $\rho_{jj}^{(2)}(r)$ densities, the sign is positive if the positive-to-negative $\rho_{jj}^{(2)}(r)$ direction is coincident with the positive direction of the chosen coordinate system, while its magnitude is proportional to their distance. The $\rho_{jj}^{(2)}(r)$ computations were performed at the CAM-B3LYP/6-31+G* level for the largest β_{xxx} and β_{zzz} components of the **3NNO** isomer, through the numerical formulation previously described in ref. 57. The $\rho_{xx}^{(2)}(r)$ and $\rho_{zz}^{(2)}(r)$ amplitudes are plotted in figure 6. In agreement with negative sign of both the β_{xxx} and β_{zzz} components, the positive to negative $\rho_{jj}^{(2)}(r)$ pairs are almost aligned along the negative directions. As can be appreciated from figure 6, for the $\rho_{xx}^{(2)}(r)$ distribution there are many similar important contributions delocalized over the entire structure. On the other hand, the largest $\rho_{zz}^{(2)}(r)$ amplitudes are mainly placed over the A, B and E rings. More importantly, the $\rho_{zz}^{(2)}(r)$ distributions are less spread out than the $\rho_{xx}^{(2)}(r)$ ones, in qualitative agreement with the relative magnitudes of the calculated hyperpolarizabilities ($|\beta_{xxx}| > |\beta_{zzz}|$, table 1).

Table 2 lists the CAM-B3LYP/6-31+G* frequency-dependent β_μ values for the SHG and EOPE NLO phenomena computed at the $\hbar\omega$ value of 0.04282 a.u. As should be expected, for both the isomers $\beta_\mu(-2\omega;\omega;\omega) > \beta_\mu(-\omega;\omega;0)$. At variance from the calculated polarizabilities, the dispersion effects on the first-order hyperpolarizabilities are different for the studied isomers. In particular, for the EOPE process the dispersion effects increases the static β_μ value of **1NNO** (**3NNO**) by 47% (43%). For the SHG phenomenon the corresponding percentages are significantly larger, being ca. 400% (**1NNO**) and 300% (**3NNO**), in part owing to resonance dispersion enhancements (the $2\hbar\omega$ value of 0.086 a.u. is rather close to the lowest-energy experimental excitation energy of 0.098 a.u.[1]). As a consequence, at $\hbar\omega = 0.04282$ a.u. the CAM-B3LYP/6-31+G* β_μ(**1NNO**)/β_μ(**3NNO**) ratios are predicted to be 1.91 and 2.41 for the EOPE and SHG processes. Note that the corresponding ratio for the static computations is calculated to be 1.87. Therefore, on the basis of the above static and dynamic $\beta_\mu(-\omega_\sigma;\omega_1,\omega_2)$ values and anticipating future experimental NLO measurements, **1NNO** might be distinguished from the **3NNO** isomer through the analysis of SHG and/or EOPE signals.

4. Conclusions

Using *ab initio* and DFT calculations, we have determined many important physicochemical properties for the **1NNO** and **3NNO** isomers, which are characterized by different mutagenic activity. The computations were performed in gas using the HF and CAM-B3LYP levels. The main results are summarized as follows: (i) The geometrical parameters, especially the typical C–C–N–O dihedral angles of the investigated isomers are close to each other. (ii) Confirming the structural data, **1NNO** and **3NNO** cannot be identified unambiguously through the IR and Raman spectra as well as the NICS(1)$_{yy}$ parameters. (iii) The ΔSCF VIE and VEA values of the title isomers are not substantially affected by position of the nitro group. Therefore, oxidation and/or reduction pathways are unable to explain the different mutagenicity of the **NNO** isomers. (iv) Owing to the mutual disposition of the polar NO_2 and N→O groups, the μ values increase on going from **1NNO** to **3NNO** by 5–7 D, depending on the level of theory. The different polarity could be related to the diverse mutagenic behaviour of the **NNO** isomers. (v) The static and frequency-dependent $\beta_\mu(-\omega_\sigma;\omega_1,\omega_2)$ values significantly decrease when passing from **1NNO** to **3NNO**, mainly due to the $\mu_z\beta_z/|\mu|$ term which roughly lies along the N→O bond of the azabenzene moiety. In future experiments, SHG and/or EOPE measurements could be used to discriminate the **NNO** isomers. (vi) In line with the recent literature findings, the long-range corrected CAM-B3LYP functional overestimates the polarizabilities and especially the first-order hyperpolarizabilities obtained by the HF calculations. (vii) The hyperpolarizability density analysis is helpful for a qualitative interpretation of the largest β_{iii} components.

References

1. Fukuhara K, Hakura A, Sera N, Tokiwa H and Miyata N 1992 *Chem. Res. Tox.* **5** 149
2. Sera N, Fukuhara K, Miyata N, Horikawa K and Tokiwa H 1992 *Mutat. Res.* **280** 81
3. Sera N, Fukuhara K, Miyata N and Tokiwa H 1994 *Mutagenesis* **9** 47
4. Chou M W, Heflich R H, Casciano D A, Miller D W, Freeman J P, Evans F E and Fu P P 1984 *J. Med. Chem.* **27** 1156
5. Tokiwa H and Ohnishi Y 1986 *Crit. Rev. Toxicol.* **17** 23
6. Fu P P 1990 *Drug Metab. Rev.* **22** 209
7. Yu H 2002 *J. Environ. Sci. Health C* **20** 149
8. Atkinson R and Arey J 1994 *Environ. Health Perspect.* **102** 117
9. Lewtas J and Nishioka M 1990 In: *Nitroarene*, Howard P, Hecht S and Beland F (eds.); pp. 61–72 (New York: Plenum Press)
10. Lewtas J, Chuang J, Nishioka M and Peterson B 1990 *Int. J. Environ. Anal. Chem* **39** 245
11. Fu P P, Chou M W, Miller D W, White G L, Heflich R H and Beland F A 1985 *Mutat. Res.* **143** 173
12. Alparone A and Librando V 2012 *Monat. Chem.* **143** 1123
13. Salafsky J S 2003 *Chem. Phys. Lett.* **381** 705

14. Velders G J M, Gillet J M, Becker P J and Feil D 1991 *J. Phys. Chem.* **95** 8601
15. Xu H-L, Li Z-R, Su Z-M, Muhammad S, Gu F L and Harigaya K 2009 *J. Phys. Chem. C* **113** 15380
16. Plaquet A, Champagne B, Castet F, Ducasse L, Bogdan E, Rodriguez V and Pozzo J-L 2009 *New. J. Chem.* **33** 1349
17. Alparone A 2012 *J. Fluorine Chem.* **144** 94
18. Katritzky A R, Pacureanu L, Dobchev D and Karelson M 2007 *J. Mol. Model.* **13** 951
19. Becke A D 1993 *J. Chem. Phys.* **98** 1372
20. Lee C, Yang A D and Parr R G 1988 *Phys. Rev. B* **37** 785
21. Hehre W J, Radom L, Schleyer P v R and Pople J A 1986 *Ab initio molecular orbital theory* (New York: Wiley)
22. Chen Z, Wannere C S, Corminboeuf C, Puchta R and Schleyer P V R 2005 *Chem. Rev*. **105** 3842 and references therein
23. Yanai T, Tew D and Handy N C 2004 *Chem. Phys. Lett.* **393** 51
24. Mills N S and Llagostera K B 2007 *J. Org. Chem.* **72** 9163
25. Ciesielski A, Krygowski T M, Cyranski M K, Dobrowolski M A and Aihara J-I 2009 *Phys. Chem. Chem. Phys.* **11** 11447
26. Alparone A 2011 *Chem. Phys. Lett.* **514** 21
27. Alparone A 2013 *J. Mol. Model.* **19** 3095
28. Medved' M and Jacquemin D 2013 *Chem. Phys.* **415** 196
29. Limacher P A, Mikkelsen K V and Luthi H P 2009 *J. Chem. Phys.* **130**(194114)
30. Zhang C-C, Xu H-L, Hu Y-Y, Sun S-L and Su Z-M 2011 *J. Phys. Chem. A* **115** 2035
31. Torrent-Sucarrat M, Solà M, Duran M, Luis J M and Kirtman B 2003 *J. Chem. Phys.* **118** 711
32. Alparone A 2013 *Chem. Phys. Lett.* **563** 88
33. Sekino H and Bartlett R J 1986 *J. Chem. Phys.* **85** 976
34. Karna S P and Dupuis M 1991 *J. Comput. Chem.* **12** 487.
35. Schmidt M W, Baldridge K K, Boatz J A, Elbert S T, Gordon M S, Jensen J H, Koseki S, Matsunaga N, Nguyen KA, Su S, Windus T L, Dupuis M and Montgomery J A Jr 1993 *J. Comput. Chem.* **14** 1347
36. Frisch M J, Trucks G W, Schlegel H B, Scuseria G E, Robb M A, Cheeseman J R, Scalmani G, Barone V, Mennucci B, Petersson G A, Nakatsuji H, Caricato M, Li X, Hratchian H P, Izmaylov A F,Bloino J, Zheng G, Sonnenberg J L, Hada M, Ehara M, Toyota K, Fukuda R, Hasegawa J, Ishida M, Nakajima T, Honda Y, Kitao O, Nakai H, Vreven T, Montgomery J A Jr, Peralta J E, Ogliaro F, Bearpark M, Heyd J J, Brothers E, Kudin K N, Staroverov V N, Kobayashi R, Normand J, Raghavachari K, Rendell A, Burant J C, Iyengar S S, Tomasi J, Cossi M, Rega N, Millam J M, Klene M, Knox J E, Cross J B, Bakken V, Adamo C, Jaramillo J, Gomperts R, Stratmann R E, Yazyev O, Austin A J, Cammi R, Pomelli C, Ochterski J W, Martin R L, Morokuma K, Zakrzewski V G, Voth G A, Salvador P, Dannenberg J J, Dapprich S, Daniels A D, Farkas O, Foresman J B, Ortiz J V, Cioslowski J and Fox D J 2009 Gaussian 09 revision A.02 Gaussian, Wallingford
37. Irikura K K, Johnson R D and Kacker R N 2005 *J. Phys. Chem. A* **109** 8430
38. Debnath A K, Lopez de Compadre R L, Debnath G, Shusterman A J and Hansch C 1991 *J. Med. Chem.* **34** 786
39. Alparone A 2012 *Monat. Chem.* **143** 513
40. Pearson R G 1993 *Acc. Chem. Res.* **26** 250
41. Chattaraj P K, Sarkar U and Roy D R 2006 *Chem. Rev*. **106** 2065, and references therein
42. McKinney J D 1989 *Environ. Health Perspect.* **82** 323
43. Fraschini E, Bonati L and Pitea D 1996 *J. Phys. Chem.* **100** 10564
44. Librando V and Alparone A 2007 *Environ. Sci. Technol.* **41** 1646
45. Mhin B J, Lee J E and Choi W 2002 *J. Am. Chem. Soc.* **124** 144
46. Hirokawa S, Imasaka T and Imasaka T 2005 *Chem. Res. Toxicol.* **18** 232
47. Librando V, Alparone A and Minniti Z 2008 *J. Mol. Struct. (Theochem)* **856** 105
48. Alparone A and Librando V 2013 *Chemosphere* **90** 158
49. Librando V, Alparone A and Tomaselli G 2008 *J. Mol. Model.* **14** 489
50. Librando V and Alparone A 2009 *J. Hazard. Mater.* **161** 1338
51. Chattaraj P K and Sengupta S 1996 *J. Phys. Chem.* **100** 16126
52. Alparone A 2013 *J. Phys. Chem. A* **117** 5184
53. Jacquemin D, Perpète E A, Medved' M, Scalmani G, Frisch M J, Kobayashi R and Adamo C 2007 *J. Chem. Phys.* **126** 191108
54. Alparone A 2013 *Chem. Phys.* **410** 90
55. Medved' M, Budzák S and Pluta T 2011 *Chem. Phys. Lett.* **515** 78
56. Nakano M, Shigemoto I, Yamada S and Yamaguchi K 1995 *J. Chem. Phys.* **103** 4175
57. Yamada S, Nakano M, Shigemoto I, Kiribayashi S and Yamaguchi K 1997 *Chem. Phys. Lett.* **267** 445
58. Nakano M, Ohta S, Tokushima K, Kishi R, Kubo T, Kamada K, Ohta K, Champagne B, Botek E and Takahashi H 2007 *Chem. Phys. Lett* **443** 95